Journal of GeoEngineering, Vol. 14, No. 4, pp. 203-217, December 2019
http://dx.doi.org/10.6310/jog.201912_14(4).1

THE SYSTEM STIFFNESS AND WALL DISPLACEMENT OF A DEEP EXCAVATION STRENGTHENED WITH CROSS WALLS IN SOFT CLAY

Hsii-Sheng Hsieh [1*], Zih-Yun Wang [2], Ting-Mei Lin [3], and Louis Ge [4]

ABSTRACT

System stiffness is an index to estimate the lateral displacement of retaining wall for deep excavations in soft clay. The original system stiffness considers two key parameters, the flexural rigidity of retaining wall and the average vertical spacing of lateral supports. However, these two parameters are unable to incorporate the effect of cross walls which are extensively used in modern day excavation projects. It is obvious that the overall stiffness of retaining system is dramatically increased with the presence of cross walls, though its amount of increment is difficult to assess. This paper devises a systematic approach to estimate the strengthening effect of cross walls on both system stiffness and the factor of safety against basal heave. The original design curves are also extended by extrapolation technique into low displacement zone that had rarely been addressed before. A deep excavation case history in soft clay is presented to demonstrate the development of these schemes. A three-dimensional numerical analysis is then used to further examine the applicability of the proposed schemes.

Key words: System stiffness, deep excavation, cross wall, wall displacement, three-dimensional effect.

1. INTRODUCTION

Estimating the displacement of retaining wall for excavations in soft clay with good accuracy is always a nuisance to most engineers. Accurate assessment of the wall displacement has its implication on the overall success of the excavation project, as the magnitude of wall displacement is linked to many issues such as the stress analysis of retaining wall, layout of lateral supports and protection of adjacent buildings. In practice, one can either resort to simple empirical equations (Ou *et al.* 1988; Woo and Moh 1990) or sophisticated numerical models (PLAXIS 2013; TORSA 2016) to perform the estimation, depending on the complexity of the excavation and budget available to the project. Empirical equation has the advantage of being simple and quick, though it is considered overly subjective and the accuracy of prediction is often questionable. On the other hand, the numerical approach is thought to be more objective and comprehensive, but its sophistication often obscures the instinct or judgment of the design engineer, which may lead to an excavation design with fatal defects.

Wide application of cross walls in recent years further complicated the issue of estimating wall displacement with accuracy, as the presence of cross walls induces pronounced three-dimensional (3D) effect that is difficult to be accounted for. It appears that excavations with cross walls can only be realistically modeled by 3D numerical tools, but for the sake of simplicity, the design engineers prefer a less sophisticated approach to estimate the possible wall displacement before they proceed further into the detailed design stage. To fulfill this purpose, a succinct scheme developed by Clough *et al*. (1989) that relies on the concept of system stiffness seems ideal. A quick estimation on the wall displacement can be achieved by using the design chart in conjunction with two parameters, one is the system stiffness (S) of the retaining structure, and the other is the factor of safety against basal heave (F_b). Unfortunately, these two parameters fail to incorporate the effects of cross walls at their present forms; therefore using Clough's original approach would overestimate the wall displacement by a wide margin.

The purpose of this paper is to revise Clough's scheme in estimating the wall displacement for excavations in soft clay with cross walls. Much of the attention is paid to incorporating the strengthening effect of cross walls on system stiffness and factor of safety against basal heave. A deep excavation case history in soft clay is presented in this paper to illustrate the development of the revised scheme. The wall displacements derived from the revised scheme are in much better agreement with the field measurements and 3D numerical results, which is regarded as an encouraging sign for further studies on the subject of system stiffness at low displacement level.

2. CLOUGH'S SCHEME TO ESTIMATE WALL DISPLACEMENT

The concept of system stiffness was first proposed by Clough *et al*. (1989) to assess the lateral displacement of retaining wall for excavations in soft clay. In their original paper, Clough *et al*.

Manuscript received February 19, 2019; revised May 3, 2019; accepted June 12, 2019.
[1*] Senior Engineer (corresponding author), Trinity Foundation Engineering Consultants, Co., Ltd., Taiwan 10685, R.O.C. (e-mail: drhsieh@tfec.com.tw).
[2] Graduate Student, Department of Civil Engineering, National Taiwan University, Taiwan 10617, R.O.C.
[3] Engineer, Trinity Foundation Engineering Consultants, Co., Ltd., Taiwan 10685, R.O.C.
[4] Professor, Department of Civil Engineering, National Taiwan University, Taiwan 10617, R.O.C.

(1989) defined the dimensionless system stiffness (S) of a retaining system as follow:

$$S = EI/\gamma_w h_{avg}^4 \quad (1)$$

where EI is the flexural rigidity of retaining wall; γ_w is the unit weight of water; and h_{avg} is the average vertical spacing of lateral supports. The lateral supports can either be basement slabs for a top-down excavation or horizontal steel bracings for a conventional bottom-up excavation. Another essential parameter in Clough's scheme to estimate wall displacement is the factor of safety against basal heave (F_b), which is basically an index incorporating the effects of undrained shear strength of soft clay (s_u) and site dimension (Terzaghi 1967). Definition of F_b is shown in Fig. 1.

Knowing the system stiffness and factor of safety against basal heave for a specific excavation, one can refer to Fig. 2 to estimate the ratio between maximum wall displacement (δ_{hm}) and excavation depth (H_e). The concept of system stiffness in conjunction with Figs. 1 and 2 serves as a good scheme to estimate the maximum wall displacement in lieu of using complex numerical tools for typical excavations in soft clay. However, with the extensive use of cross walls in modern day excavations (Ou *et al.* 2006; Hsieh *et al.* 2008), this approach has inherent shortcomings as it is unable to model the effect of cross walls or the 3D effect of small sites (Hsieh *et al*. 2015). It is also noted that most urban excavations in soft clay adopt diaphragm wall as the retaining structure to reduce wall displacement in an effort to minimize the impact of

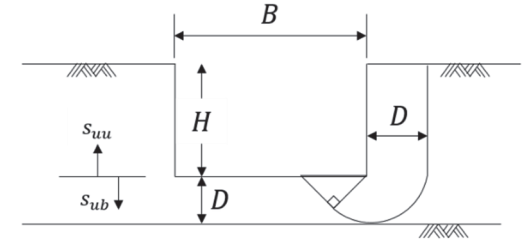

$$FS = \frac{1}{H}\frac{N_c s_{ub}}{\gamma - s_{uu}/D}$$

(a) $D < (\sqrt{2}/2)B$

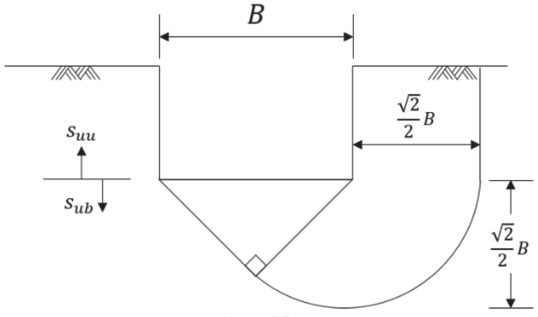

$$FS = \frac{1}{H}\frac{N_c s_{ub}}{\gamma - \frac{2}{\sqrt{2}}\frac{s_{uu}}{B}}$$

(b) $D > (\sqrt{2}/2)B$

Fig. 1 Factor of safety against basal heave (Terzaghi 1967)

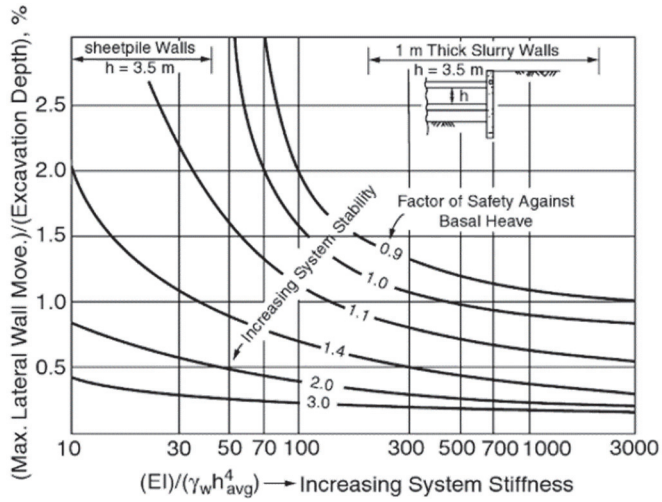

Fig. 2 Relationship between maximum wall displacement and system stiffness (Clough *et al.* 1989)

excavation on adjacent buildings. For diaphragm wall with a minimal thickness of 0.6m and a specified concrete strength of 27.5 MPa, the flexural rigidity of diaphragm wall generally exceeds 4.5E+05 kN-m^2. Given a typical support spacing (h_{avg}) of 3.5 m, the system stiffness of modern day excavation is in general higher than 300 (S > 300), which implies that the left portion of Fig. 2 with S less than 300 is virtually useless for modern day excavations. Furthermore, modern day excavations in urban area often have stringent limit on wall displacement that would necessitate the maximum wall displacement being controlled roughly within 0.3% of the excavation depth when safety of adjacent buildings is of concern. With such a stringent requirement on wall displacement, most curves shown in Fig. 2 become obsolete. It is therefore apparent that Clough's original scheme to estimate the excavation induced wall displacement in soft clay has to be enhanced or overhauled for modern day excavations.

3. AN EXCAVATION CASE HISTORY IN SOFT CLAY

3.1 Project Description

A case history is presented in this section as an example to reveal the inherent shortcomings of Clough's original scheme. This case history locates at Shih-Lin District of Taipei City, which is an area notorious for its thick soft clay deposit and high ground water table. The project site was originally occupied by a deteriorating 7-story building that the owners decided to demolish and replace it with a 14-story high-rise residential building. To fulfill parking requirement of the new building, a 4-story basement reaching an excavation depth of 16 m is needed. Not surprisingly, the project site is surrounded by existing buildings at close proximity (Fig. 3). Some of the adjacent buildings are in terrible shape, either tilting significantly toward the project site or with concrete blocks falling off the floor slab. With this in mind, the project owner and contractor are very conservative about excavating within this thick soft clay deposit, therefore they asked the structural engineer to be extra careful on the foundation and excavation design.

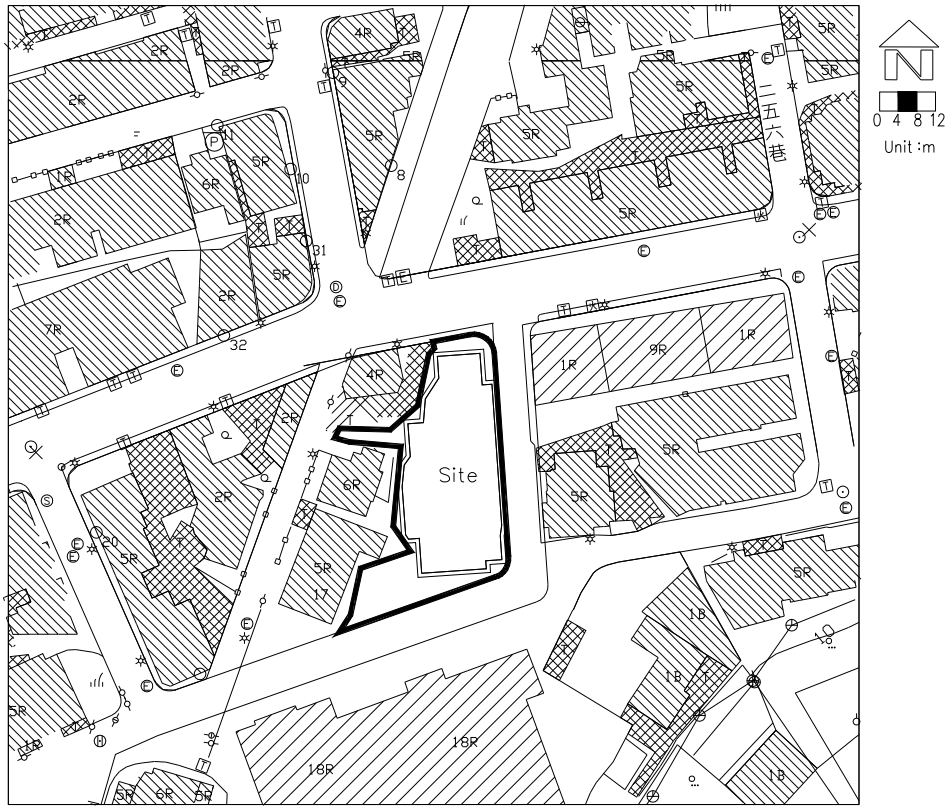

Fig. 3 Site plan

3.2 Ground Condition

Site investigation results show that the project site is covered by a 3.4 m thick surface fill, followed by a thick soft clay deposit to a depth varying from GL.–19 m to GL.–30 m. The Standard Penetration Test N values (SPT N) of this clay deposit increase from 2 at GL.–3.4 m to about 4 at the bottom elevation. The average natural water content and liquid limit of clay samples are 46% and 48%, respectively. Undrained shear strength (s_u) of this soft clay is considered to increase with the effective overburden pressure (σ_v'), and a ratio of 0.24 is used between s_u and σ_v', *i.e.*, $s_u = 0.24\sigma_v'$. Underlain the soft clay layer is a very dense layer comprises mainly of andesite debris. SPT N values of this very dense layer are more than 50, and it is regarded as the bearing stratum of the project site. The depth of andesite debris governs the foundation and excavation design and the depth contour of the andesite debris is shown in Fig. 4. Essential physical and engineering parameters of each layer are listed in Table 1.

Table 1 Simplified soil profile

Layer	Soil Type	Depth (GL.–m)	SPT N	γ_t (kN/m³)	s_u (kN/m²)	c' (kN/m²)	ϕ' (°)
1	SF	0 ~ 3.4	4	17.0	–	0.0	28
2	CL / CH	3.4 > 19	2 ~ 4	17.2	$0.24\sigma_v'$	0.0	28
3	Andesite	> 19	>50	23.0	–	0.0	38

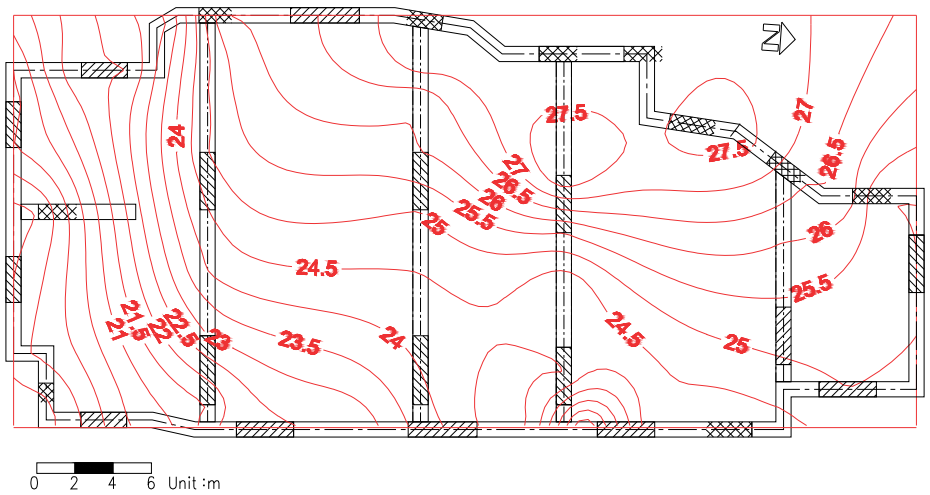

Fig. 4 Depth contour of andesite debris

Ground water level was found at about 2 m below surface. Piezometers installed within the andesite debris revealed that the ground water is in a static state rather than under artesian pressure, which is fortunate for the design and field engineers to deal with one less nemesis.

Other than the soft clay deposit, one more obstacle to the construction project is a large portion of the site is occupied by the old basement of the demolished structure. The existence of the old basement poses as a barrier to the construction of diaphragm wall, leading to a 4-month delay on the construction schedule as the construction crew fought through the concrete and steel of the old basement to erect deep guide walls for diaphragm wall and cross walls construction at a very slow pace. To facilitate the construction of these deep guide walls, most part of the old basement was demolished and later backfilled with brick or concrete rubbles once the guide walls were completed. Since the old basement was virtually removed before excavation, it had insignificant effect on the measured wall displacements during excavation stage of the new basement.

3.3 Retaining System

The excavation design utilizes a perimeter diaphragm wall 0.8 m in thickness, which extends from ground surface and penetrates 1.5 m into the bearing layer. Referring to depth contour of andesite shown in Fig. 4, the total length of diaphragm wall varies from 21 m to 30 m depending on the depth of the andesite layer. Embedment in the dense andesite debris is necessary as the diaphragm wall is required to provide adequate passive resistance to counter the active earth pressure on the retaining side. The diaphragm wall also serves as an integral part of the foundation system as it carries structural loads through columns embedded in the diaphragm wall. Four levels of horizontal bracing were installed stage by stage in a conventional bottom-up staged excavation. The horizontal bracing consists of H-section steel beams that were prestressed to design values immediately after installation. Plan layout and profile of the bracing system are shown in Figs. 5 and 6, respectively. Details including dimension and installation depth of steel beams are listed in Table 2. It is noted that the bracing design is overly conservative in an apparent effort to guard against all adversities.

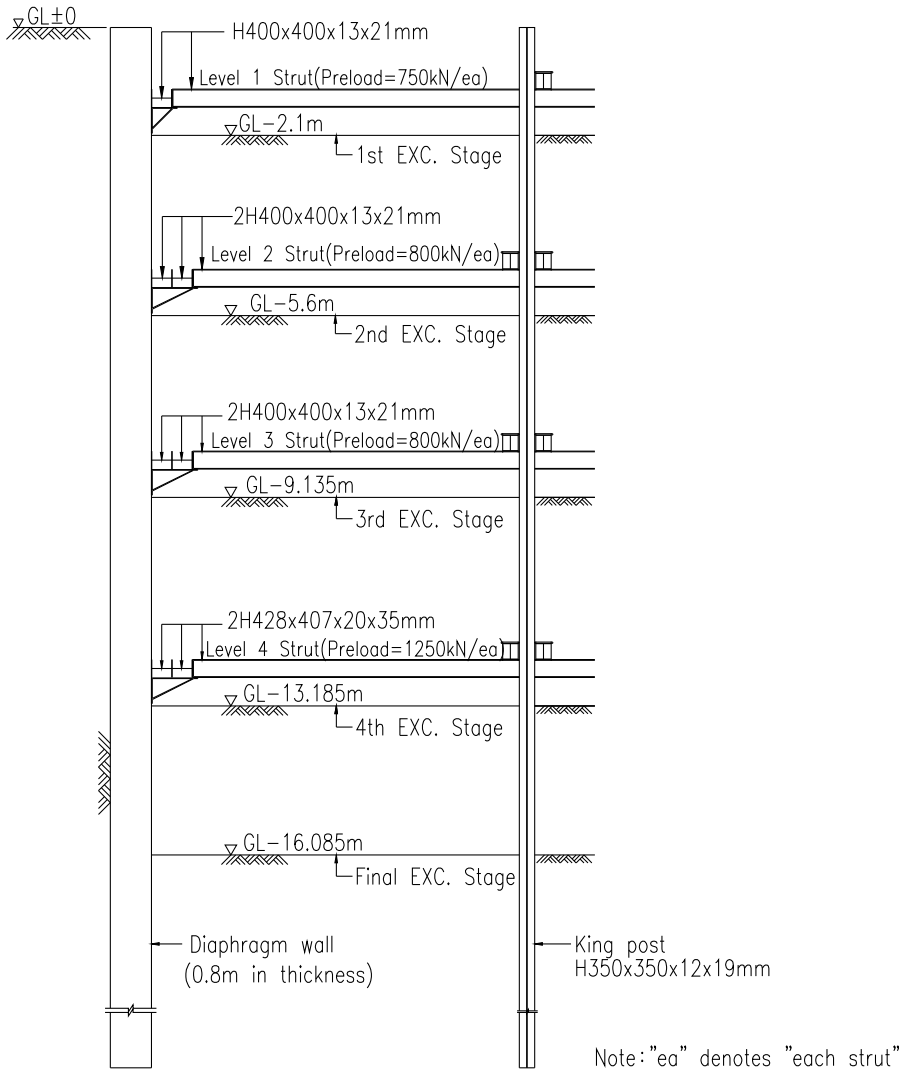

Fig. 5 Excavation profile

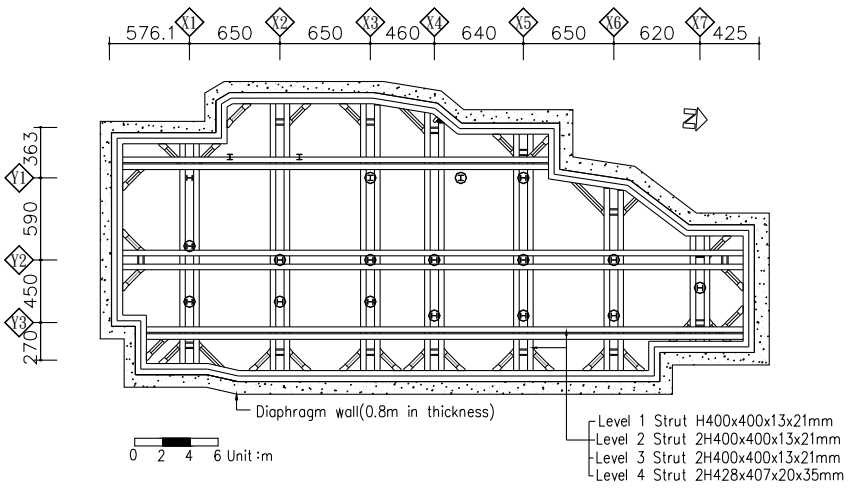

Fig. 6 Plan layout of bracing system

Table 2 Details of horizontal bracing system

Level	Strut Dimension(mm)	Preload (kN/each strut)	Depth
1	H400 × 400 × 13 × 21	750	GL–1.2m
2	2H400 × 400 × 13 × 21	800	GL–4.7m
3	2H400 × 400 × 13 × 21	800	GL–8.2m
4	2H428 × 407 × 20 × 35	1250	GL–12.3m

To further strengthen the retaining system, four cross walls as shown in Fig. 7 were constructed. The thicknesses of the cross walls are the same as the perimeter diaphragm wall, and both walls were constructed with the same equipments at the same time. All cross walls were embedded in dense andesite debris for at least 1.5 m and cast to a depth of 2.1 m below ground surface, which is the depth of the first excavation stage. The cross walls were demolished step by step to the dredge line of each excavation stage in order that the horizontal bracing system can be erected without obstructions. These cross walls are dual purpose walls because they not only provide extra horizontal supports to the retaining system, but also behave as load bearing piles for the 14-story building.

3.4 Field Measurement of Wall Displacement

A total of six inclinometer casings (SI) were installed within the perimeter diaphragm wall to measure the wall displacement. Location of the inclinometer casings are shown in Fig. 7. Displacement curves of the diaphragm wall for the final excavation stage were shown in Fig. 8, revealing that the maximum wall displacement (δ_{hm}) for all inclinometer casings is less than 5 mm, which is less than 0.03% of the excavation depth. The observed wall displacement is extremely low from a practical point of view and is well underneath Clough's lowest design curve with $F_b = 3$. Construction experience accumulated over the past decades indicates that the maximum wall displacement (δ_{hm}) for deep excavation in clay roughly falls within 0.5% to 1.2% of the excavation depth (Ou *et al*. 1988; Woo and Moh 1990). For this particular project with $s_u = 0.24\ \sigma_v'$, δ_{hm} is approximately 0.9% of the excavation depth, which corresponds to 144 mm for an excavation depth of 16 m. Compared with field measurements, the empirical δ_{hm} value is about 30 times the observed value (144 mm *vs.* 5 mm), and it is obvious that the strengthening effect of cross walls on retaining system should not be overlooked.

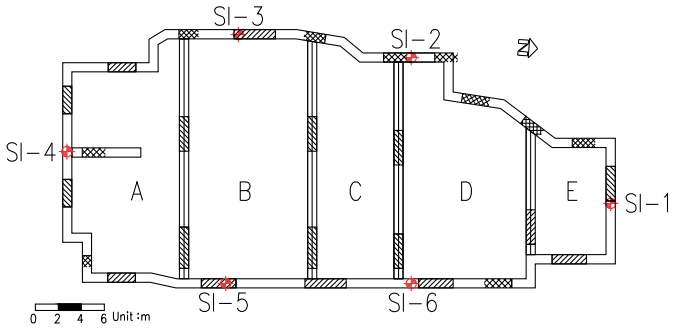

Fig. 7 Layout of cross walls and location of inclinometer casings

Another feature worth mentioning is that some inclinometer casings (SI-4, SI-5, and SI-6) showed negative wall displacement at top of the diaphragm wall. One may suspect that the bottom of diaphragm wall might have moved inward, resulting in an inaccurate interpretation on the displacement readings of inclinometer casings. This possibility is ruled out because all diaphragm wall panels were embedded in bearing stratum that the lateral and vertical movements at bottom of the diaphragm wall were refrained. Another possible scenario is the preload of horizontal bracing system exceeded the active force acting on the retaining side of the diaphragm wall for the first two stages of excavation; therefore, top portion of the diaphragm wall was pushed outward by the bracing system. This phenomenon rarely occurs for large excavation site, but it is not impossible to happen for small site with good workmanship on bracing system and high preload level of the bracing system.

4. REVISION OF CLOUGH'S SCHEME

4.1 Use of the Original Scheme

Instead of using a rough empirical equation, Clough's scheme described in Section 2 is adopted to estimate the wall displacement of this case history. Clough's scheme is considered as a more systematic and objective approach as it uses parameters that incorporate structural and geotechnical factors in calculating the wall displacement. Ignoring the effect of cross walls, the wall displacement of this particular project is estimated below.

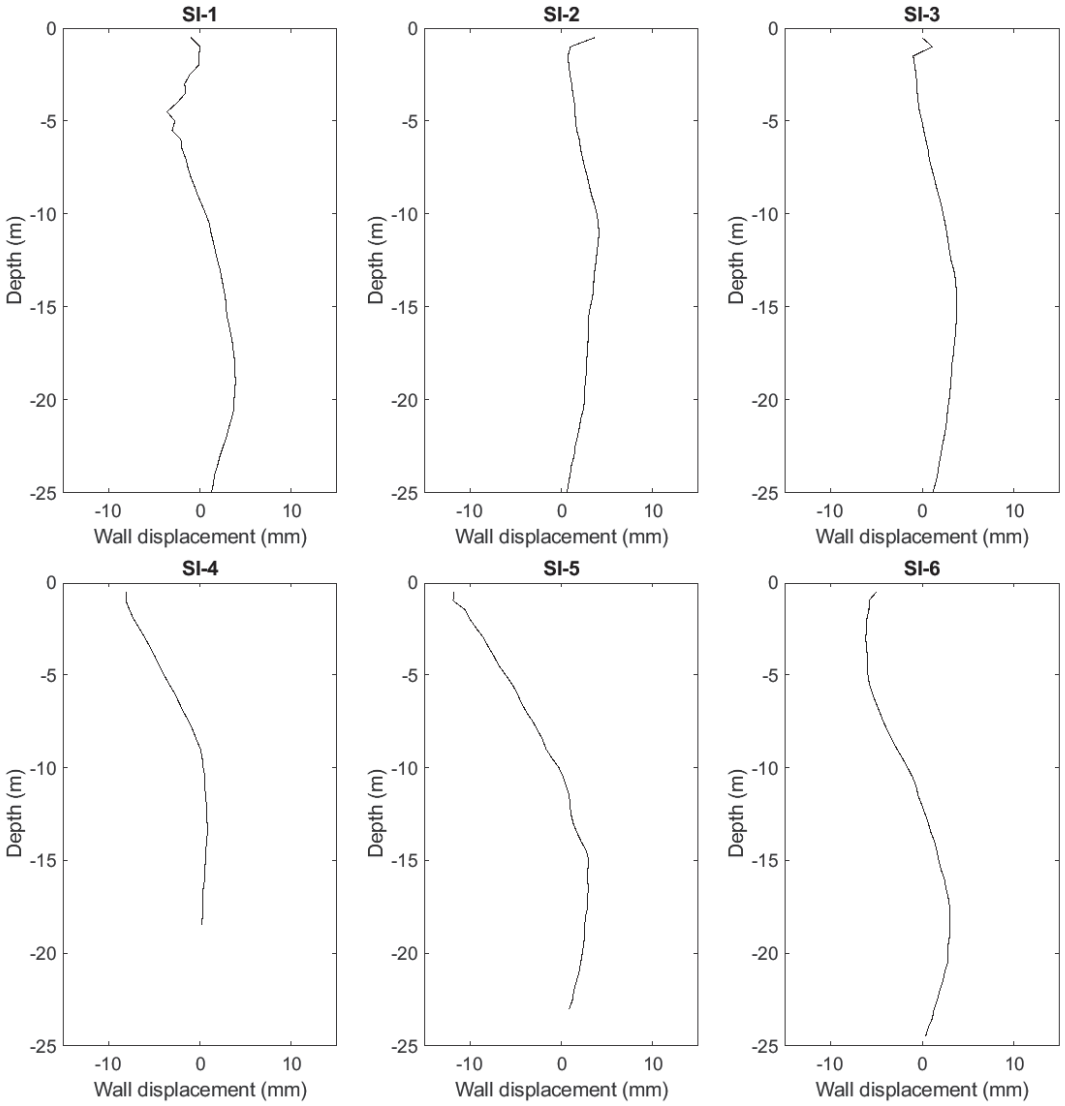

Fig. 8 Displacement of diaphragm wall at end of excavation

With a wall thickness of 0.8 m and a specified concrete strength of 27.5 MPa (280 kg/cm^2), the flexural rigidity (EI) of the diaphragm wall is 1.05E+06 KN-m^2. The average vertical spacing of struts (h_{avg}) is 3.55 m as shown in Fig. 5. Inserting these numbers into Eq. (1) yields a dimensionless system stiffness (S) of 675 for this case history. Since the corresponding site width (B), depth of bearing stratum, and the average undrained shear strength below dredge line (s_{ub}) are all different at the location of each inclinometer casing, the factor of safety against basal heave (F_b) is not a fixed number for this site. The F_b value for each inclinometer casing together with the estimated wall displacement (δ_{clough}) and field measurement (δ_{field}) are listed in Table 3. Comparing the estimated wall displacements and field measured data, it is self evident that Clough's scheme over estimates the wall displacements by a significant margin with the effects of cross walls unaccounted for.

Since cross walls are gaining popularity among design engineers as a main component of the excavation design and knowing that Clough's original scheme is unable to cover the effect of cross walls in limiting wall displacement, there is a dire need to revise the original scheme. Intuitively, cross walls provide additional passive resistance to the retaining system, and the overall system stiffness and basal stability are both increased as a result.

Table 3 Estimated wall displacement by Clough's scheme

SI	Zone	B (m)	D (m)	s_{uu} (kN/m^2)	s_{ub} (kN/m^2)	F_b (–)	δ_{hm}/H_e (%)	δ_{clough} (mm)	δ_{field} (mm)
1	E	6	8.9	14.15	35.84	0.92	1.30	209.30	3.90
2	D	15	13.9	14.15	40.07	0.90	1.10	177.10	4.11
3	B	18	11.9	14.15	38.38	0.85	1.28	206.08	3.78
4	A	10	2.9	14.15	30.75	0.89	1.10	177.10	0.83
5	B	18	6.4	14.15	33.72	0.80	1.30	209.30	3.01
6	D	15	7.9	14.15	34.99	0.81	1.30	209.30	3.04

Note: Please refer to Fig.1 for the definition of B and D in estimating F_b

If the effects of cross walls on system stiffness and basal stability can be reasonably quantified, there is a good chance that Clough's scheme can be extended into the area where the wall displacement is at extremely low level.

Also worth noting for this particular excavation case is that to ignore the embedment of diaphragm wall in andesite debris seems to underestimate the factor of safety against basal heave, though the factor of safety against basal heave shown in Fig. 1 is not a function of the embedment depth of retaining wall. Intuitively, the 1.5m embedment of diaphragm wall in andesite debris helps in limiting the wall displacement, but this beneficial effect of

embedment may already be included in the factor of safety against basal heave as the parameter D shown in Fig. 1 for the calculation of F_b is related to the depth of andesite debris. Andesite debris at shallow depth requires that the retaining wall be adequately embedded in this dense layer, while at the same time the value of F_b is increased as result of the smaller D parameter. In summary, the effect of wall embedment in andesite debris is intrinsically incorporated in the calculation of F_b.

4.2 Revision of the System Stiffness

By visual inspection of the cross wall layout shown in Fig. 7, the project site is subdivided by cross walls into five small sectors marked with A through E, respectively. Each sector is so small that pronounced 3D or corner effect prevails. In other words, the retaining system is greatly strengthened by the cross walls and lateral wall displacement is significantly reduced by 3D or corner effect as a result. Estimating the wall displacement under the influence of 3D effect can be a formidable task. Mind boggling and time consuming 3D numerical analyses may have to be engaged to tackle such problems. Though simplified approaches had been proposed to model the behavior of cross walls (Hsieh and Lu 1999) and 3D effect of small sites (Hsieh *et al*. 2015), these approaches still involve the use of one-dimensional (1D) numerical program that could be a problem for inexperienced engineers.

Instead of using complex numerical programs, this paper resorts to simple chart to quantify the 3D effect induced by the presence of cross walls. Figure 9 is a chart proposed by Ou *et al.* (1996), in which the plane strain ratio (*PSR*) is defined as the ratio between the maximum wall displacement under 3D effect and the maximum wall displacement under plane strain condition. The *PSR* at any location of the perimeter diaphragm wall can be obtained by entering the site dimension and distance from the corner. As a hypothesis for excavation with cross walls, the junctions of cross walls and perimeter wall are also regarded as corners, therefore, the *PSR* of each sectors dissected by cross walls as shown in Fig. 7 can be estimated by the use of Fig. 9. In this study, the *PSR* at midpoint of each sector is used to represent the 3D effect of that particular sector, though the inclinometer casing is not necessarily located at the midpoint. The *PSR* is a reduction factor for wall displacement by definition and its inverse is considered as the magnification factor of the original system stiffness in this paper. The combined system stiffness (S_c) as a combination of the original system stiffness and the corner or 3D effect induced by cross wall is therefore defined as:

$$S_c = \frac{S}{PSR} \tag{2}$$

where S_c is the combined system stiffness which is a dimensionless factor the same as S.

As an alternative, *PSR* can also be calculated by the equation proposed by Finno *et al.* (2007), which can be easily inserted in a spreadsheet for quick calculation. However, this paper opts to use Fig. 9 to determine the *PSR* so perhaps the engineers can better follow the process that requires a step-by-step hand calculation by human.

Hypothesizing the junction of cross wall and perimeter diaphragm wall as corner enables the authors to utilize the *PSR* concept proposed by Ou *et al.* (1996), though cross walls were demolished stage by stage and the junctions did not totally resemble the true corner of a typical site. However, in the field practice, the

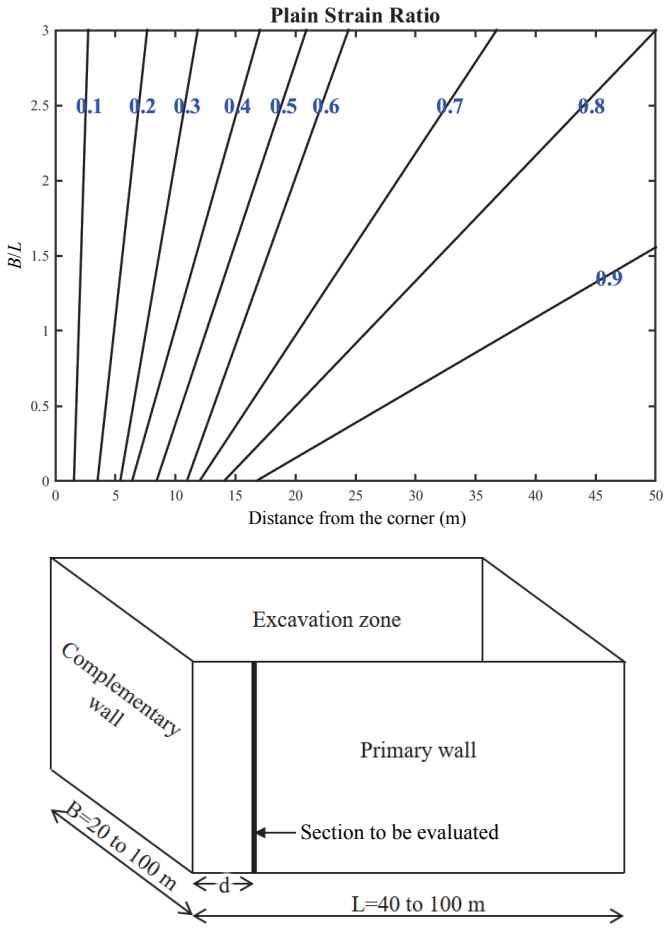

Fig. 9 Plane strain ratio (Ou *et al.* 1996)

demolished part of cross wall is promptly replaced with horizontal bracing with adequate preload, that refrains the diaphragm wall above dredge line from developing noticeable inward movement at junction point. Below the dredge line, the cross wall is yet to be demolished, and the existence of cross wall effectively minimizes the inward movement of diaphragm wall at junction point. Combining the refraining effects of bracing above dredge line and cross wall below dredge line, the inward movement of diaphragm wall at junction point remains insignificant, and that allows the authors to consider the junction point to behave close to a corner.

4.3 Revision of the Factor of Safety against Basal Heave

Having calibrated the original system stiffness by incorporating the 3D effect of cross walls, the next issue is how the factor of safety against basal heave (F_b) can also be adjusted. In physical sense, the cross walls not only provide additional lateral resistance to the retaining system, but also serve to refrain the development of basal heave failure surface shown in Fig. 1. When the soft clay bounded between cross walls begins to move upward in the heaving process during excavation, side frictions developed between cross walls and soft clay act as additional resistance to counter basal heave. It is assumed that the magnitude of side friction is the adhesion between cross walls and soft clay, and for simplicity, magnitude of the adhesion is assumed the same as the undrained shear strength of clay (s_u). Hypothesizing that the total adhesion provided by the cross walls can be deduced to an increase in s_{ub},

the equivalent undrained shear strength of clay beneath dredge line on the excavation side can be calculated and inserted into the equations shown in Fig. 1 to compute the adjusted factor of safety against basal heave (F_{b_adj}). In mathematical forms:

$$s_{ub}^{*} = s_{ub}(1+\beta L_{cw} N_{cw} / L) \quad (3)$$

where s_{ub}^{*} is the equivalent undrained shear strength beneath dredge line on the excavation side incorporating the effect of cross walls; β is a factor generally taken as two since adhesion developed on both sides of a single cross wall; L_{cw} is the length of cross wall; N_{cw} is the number of cross walls; and L is length of perimeter diaphragm wall reinforced by the cross walls. It is clearly indicated in Eq. (3) that s_{ub}^{*} is a function of the number and length of cross walls. Intuitively, the longer the cross wall and the more the cross walls are both beneficial to the increment of s_{ub}^{*}, which is consistent with the content of Eq. (3). Length of cross wall is a fixed design value relating to the dimension of project site, but the number of cross walls can be increased if a high s_{ub}^{*} is desired in the design. Details on the derivation of equivalent undrained shear strength (s_{ub}^{*}) can be found in Hsieh and Lu (1999) and TORSA3 user manual (2019).

It has to be pointed out that in this study, F_{b_adj} is calculated for each small sector dissected by cross walls, therefore L is the width of that small sector; L_{cw} is the length of cross wall at the location of that particular sector; N_{cw} is taken as two because there are two cross walls for a small sector; and β is taken as unity since the adhesion of a cross wall is shared by two adjacent sectors. It is noted that the project site is dissected by cross walls into small sectors and adjacent sectors are bordered by a common cross wall, the strengthening effect of a particular cross wall is shared by these two adjacent sectors and therefore β is taken as unity instead of two as stated in the previous paragraph. Another issue worth noting is the s_{ub_adj} value used to calculate F_{b_adj} is the average value of the original s_{ub} and s_{ub}^{*} as the cross walls affect only the clay strength on the excavation side and the clay strength on the retaining side remains the same, *i.e.*, $s_{ub\_adj} = (s_{ub} + s_{ub}^{*})/2$.

As stated in the original paper (Clough *et al*. 1989), the factor of safety against basal heave is used instead of the simple stability number for correlation with wall movement since it can account for the effects of more variables, including depth to a rigid base and the width and shape of the excavation. In this study, the effect of cross wall is considered as one additional variable to be included in the factor of safety against basal heave to calibrate the wall movement. Hypothesizing the effect of cross wall as an increase of s_{ub} and adjusting the factor of safety against basal heave accordingly is in line with the idea of the original paper. In essence, the factor of safety against basal heave is mainly used as an index parameter to correlate the wall movement rather than being regarded as a bearing capacity related factor.

4.4 Extrapolation of Design Curves

The original design curves shown in Fig. 2 are applicable for sites with system stiffness less than 3000 ($S < 3000$) and factor of safety against basal heave less than 3 ($F_b < 3$). With the presence of cross walls, the S and F_b values can exceed the limits if these two factors are adjusted according to the approaches outlined in the above sections. Therefore, the original design curves have to be extended to cover the area with high S and F_b values. Rather than to reconstruct the design curves by sophisticated 3D simulations such as the research conducted by Bryson and Zapata-Medina (2012), this paper resorts to a simple curve fitting technique to extend the design curves further into the low displacement area.

Re-plotting Fig. 2 with F_b as the X-axis, the relationship between δ_{hm} / H_e, S and F_b is redrawn and shown in Fig. 10. The curves in Fig. 10 for F_b less than 3 are plotted with the original data from Fig. 2, and these curves can be extrapolated to high F_b values by curve fitting technique. It is interesting to note that those curves in Fig. 10 can be represented by a simple equation in the following form:

$$\delta_{hm} / H_e = \alpha F_b^{-1.55} \quad (4)$$

where α is a factor depending on the value of system stiffness. With the α values shown in Fig. 10, the relationship between α and S is further investigated and another simple equation can be obtained (Fig. 11):

$$\alpha = 2.17 S^{-0.143} \quad (5)$$

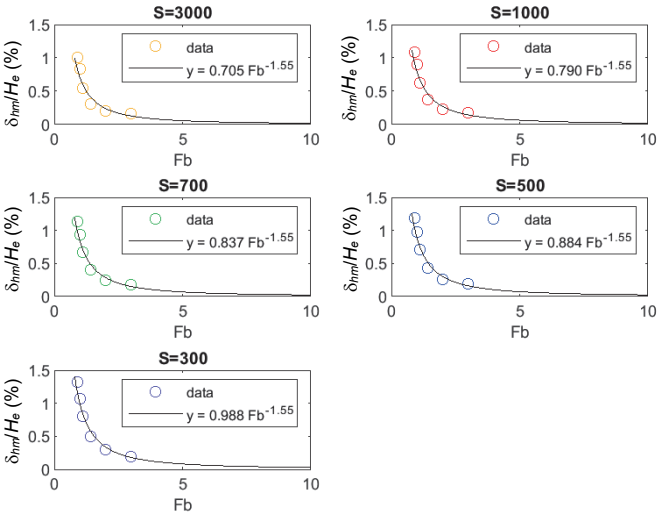

Fig. 10 Extrapolation of the design curves

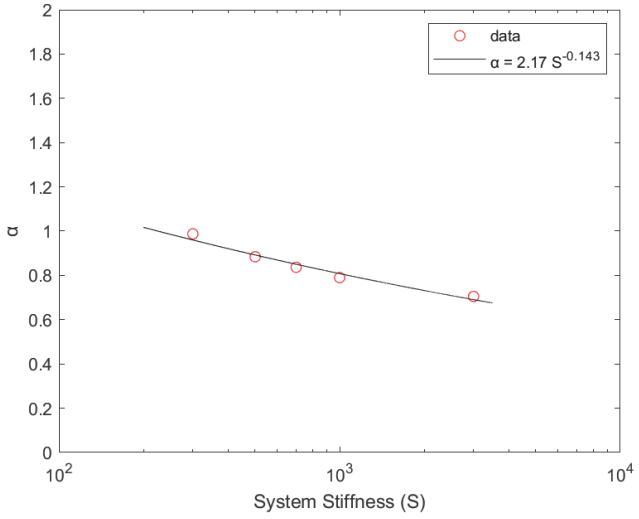

Fig. 11 Relationship between *α* and *S*

Combining Eqs. (4) and (5), a succinct equation representing the relationship between ratio of wall displacement (δ_{hm}/H_e), system stiffness (S) and factor of safety against basal heave (F_b) can be established, which assumes the following form:

$$\delta_{hm} / H_e = 2.17 S^{-0.143} F_b^{-1.55} \quad (6)$$

Since the derivation of Eq. (6) is based upon the curves shown in Fig. 10, the applicable ranges of Eq. (6) is currently limited to $F_b \geq 0.9$ and $S \geq 300$. Using the extrapolated curves in Fig. 10 or Eq. (6) as a basis, Fig. 2 can be expanded to include curves with high F_b values. As shown in Fig. 12, three more curves with F_b = 5, 7, and 10, are added to Clough's original graph. These three curves occupy the lower right corner of Fig. 12 and are apparently inconspicuous when compared with other curves at lower F_b values. In order to have a better visual effect, curves at the lower right corner of Fig. 12 are redrawn with an arithmetic scale and the results are shown in Fig. 13.

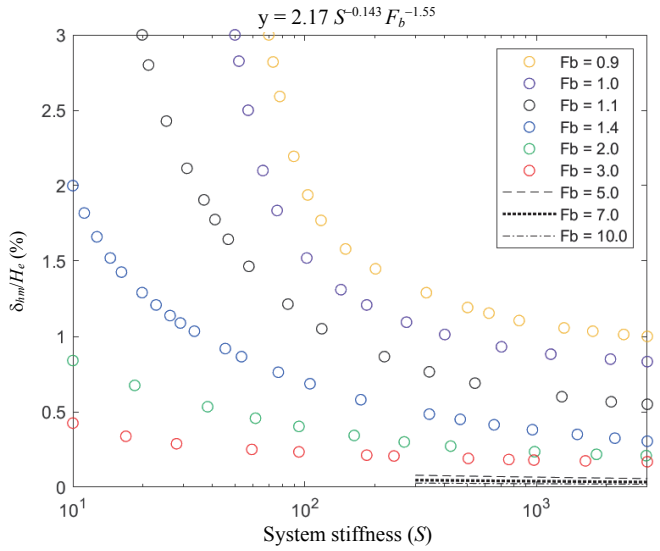

Fig. 12 Additional of design curves with F_b = 5, 7, and 10

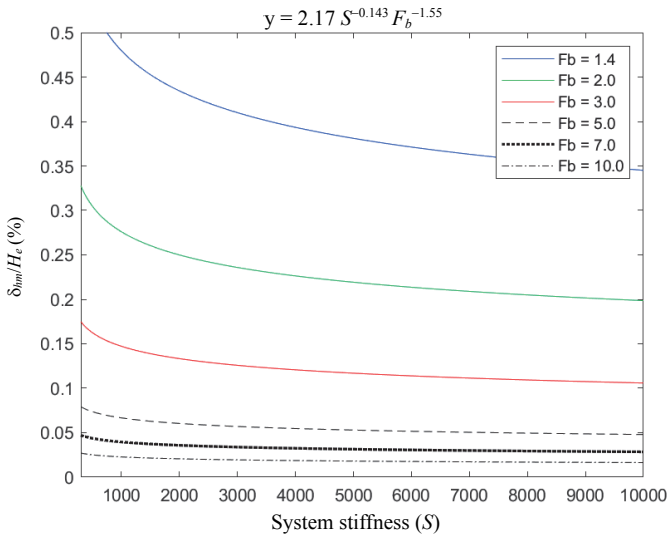

Fig. 13 Design curves with F_b > 0.9 and S > 300

Inspecting these additional curves in Fig. 13, it appears that the relationship between δ_{hm}/H_e and S is almost linear for $F_b \geqq 3$ and $S \geqq 3000$. More specifically, δ_{hm}/H_e values fall within a small range between 0.02% and 0.12% for $F_b \geqq 3$ and $S \geqq 3000$. In other words, if the excavation design incorporates adequate number of cross walls to fulfill both $F_b \geqq 3$ and $S \geqq 3000$, it is possible to limit the lateral displacement of retaining wall to less than 0.12% of the excavation depth. On the other hand, Fig. 13 also implies that there is at least a 0.02% of δ_{hm}/H_e even if the excavation is heavily reinforced with a large number of cross walls.

4.5 Re-evaluating Wall Displacements of the Case History

Following the schemes presented in the above sections to account for the effects of cross walls, the combined system stiffness (S_c) and adjusted factor of safety against basal heave (F_{b_adj}) are calculated, and the results are listed in Tables 4 and 5. The S_c values shown in Table 4 are function of the original system stiffness and *PSRs*. With the cross walls provide pronounced 3D or corner effect for the project site, the *PSRs* may reach a low value in the vicinity of 0.15, which means the system stiffness may be augmented by a factor 6.7 as shown in Table 4. In real numbers, the system stiffness had increased from the original value of 675 to a revised value of 4497.

Once the combined system stiffness and adjusted factor of safety against basal heave corresponding to the location of each inclinometer casing had been calculated, the δ_{hm} of each inclinometer casing can be revised according to Fig. 13 or Eq. (6). The original and revised δ_{hm} together with the field measurements are presented in Table 6 for comparison. It appears that the revised predictions on wall displacement (δ_{rev}) are much closer to the measured values (δ_{field}) compared to those based on the original Clough's scheme (δ_{Clough}). Though the revised predictions on wall displacement (δ_{rev}) are still far away from the measured values (δ_{field}), the revised scheme is nonetheless considered a breakthrough in predicting wall displacements for excavations with cross walls.

Table 4 Combined system stiffness of the case history

SI	Zone	B (m)	L (m)	S (–)	PSR (–)	S_c (–)
1	E	6	7.5	675	0.15	4497
2	D	15	11	675	0.22	3066
3	B	18	10	675	0.18	3748
4	A	10	14.5	675	0.32	2108
5	B	18	10	675	0.18	3748
6	D	15	11	675	0.22	3066

Note: Please refer to Fig. 9 for the definition of B and L in estimating *PSR*

Table 5 Adjusted factor of safety against basal heave

SI	Zone	N_{cw} (m)	L_{cw} (m)	β (–)	L (m)	s_{uu} (kN/m^2)	s_{ub_adj} (kN/m^2)	F_b (–)	F_{b_adj} (–)
1	E	2	6	2	7.5	14.15	93.18	0.92	2.39
2	D	2	15	1	11	14.15	94.72	0.90	2.12
3	B	2	18	1	10	14.15	107.46	0.85	2.38
4	A	2	12	2	14.5	14.15	81.66	0.89	2.35
5	B	2	18	1	10	14.15	94.41	0.80	2.24
6	D	2	15	1	11	14.15	82.70	0.81	1.91

Table 6 Comparison of the wall displacements

SI	S (–)	S_c (–)	F_b (–)	F_{b_adj} (–)	δ_{clough} (mm)	δ_{rev} (mm)	δ_{field} (mm)
1	675	4497	0.92	2.39	209.30	27.25	3.90
2	675	3066	0.90	2.12	177.10	34.60	4.11
3	675	3748	0.85	2.38	206.08	28.04	3.78
4	675	2108	0.89	2.35	177.10	31.01	0.83
5	675	3748	0.80	2.24	209.30	30.93	3.01
6	675	3066	0.81	1.91	209.30	40.80	3.04

The obvious discrepancies between the revised predictions on wall displacement (δ_{rev}) and the measured values (δ_{field}) can perhaps be attributed to various construction factors cannot be fully accounted for in this study, such as excellent workmanship of the bracing system and a carefully implemented excavation plan. Based upon the authors' experience, the measured wall displacements are far too low compared with other sites with similar conditions. Though it is fortunate to control the actual wall displacement within a small value, the excavation design should use a conservative value such as δ_{rev} to ensure the safety of the entire project.

5. THREE-DIMENSIONAL NUMERICAL ANALYSES

Three-dimensional numerical analysis is considered the most straightforward approach to simulate a complex excavation. In this study, a 3D numerical model was established using PLAXIS software to calculate the wall displacement of the case history. Rather than to pursuit a perfect simulation of the excavation, this PLAXIS analysis emphasized on the sensitivity studies of pivotal parameters such as undrained shear strength of clay and axial stiffness of bracings. Results of the numerical analyses can be used to validate the revised scheme outlined in the previous section and to delineate the importance of cross walls in limiting wall displacement.

5.1 Basic Information of 3D Analyses

Figure 14 shows the finite element model of the project site with a plan dimension of about 47 m by 18 m, which is only a small part of the whole PLAXIS 3D analysis domain. Soil parameters of each layer are listed in Table 7 and elasto-plastic Mohr-Coulomb model is selected to simulate the soil behavior. In the 3D numerical analysis, clay layers are treated as undrained materials while ground water level in the permeable andesite debris on the excavation side is lowered to 1m below dredge line in each excavation stage. Parameter of structural elements, including diaphragm wall and cross walls are listed in Table 8. The excavation sequence is presented in Table 9.

Once the combined system stiffness and adjusted factor of safety against basal heave corresponding to the location of each inclinometer casing had been calculated, the δ_{hm} of each inclinometer casing can be revised according to Fig. 13 or Eq. (6). The original and revised δ_{hm} together with the field measurements are presented in Table 6 for comparison. It appears that the revised predictions on wall displacement (δ_{rev}) are much closer to the measured values (δ_{field}) compared to those based on the original Clough's scheme (δ_{Clough}). Though the revised predictions on wall displacement (δ_{rev}) are still far away from the measured values (δ_{field}), the revised scheme is nonetheless considered a breakthrough in predicting wall displacements for excavations with cross walls.

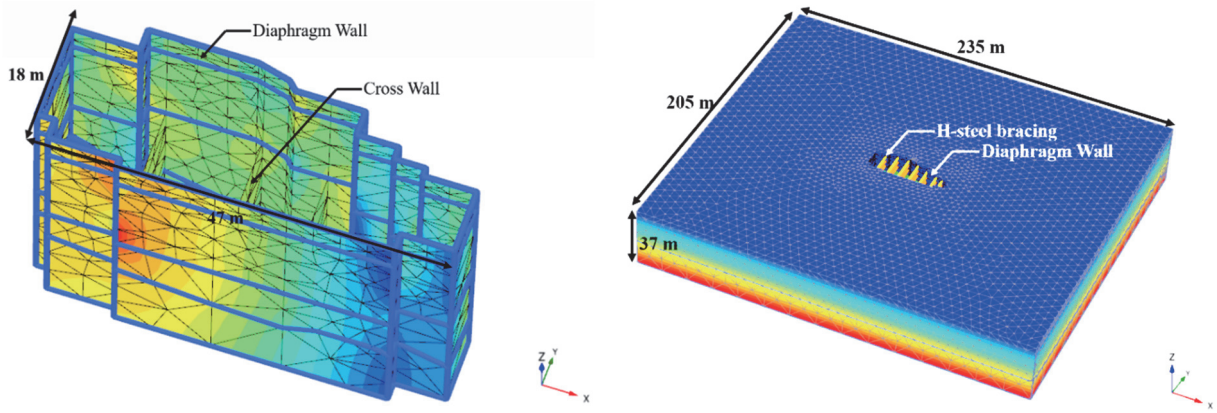

(a) Model of the retaining wall system (b) Analysis domain

Fig. 14 Finite element mesh of the 3D simulation

Table 7 Material properties of the soil layers

Type	Depth from (m)	Depth to (m)	γ_t (kN/m^3)	SPT N (–)	c' (kPa)	ϕ' (°)	s_u (kPa)	E (kPa)	ν_u (–)	R_{int} (–)
1SF	0.0	– 3.4	17.0	4	0	28		8000	0.3	0.67
2CL	– 3.5	– 4.0	17.2	2	0	0	7.79	3897	0.495	0.67
2CL	– 4.0	– 12.0	17.2	2	0	0	21.35	10677	0.495	0.67
2CL	– 12.0	– 18.0	17.2	3	0	0	31.53	15763	0.495	0.67
2CL	– 18.0	– 20.0	17.2	3	0	0	34.92	17458	0.495	0.67
2CL	– 20.0	– 23.0	17.2	4	0	0	40.00	20001	0.495	0.67
3Andesite	– 23.0	– 30.0	23.0	> 50	0	38		912000	0.3	0.67

Table 8 Material properties of the diaphragm wall (DW) and cross wall (CWa and CWb)

Type	Depth from (m)	Depth to (m)	Thickness (m)	fc' (MPa)	E (kPa)	I (m^4)	v (–)
DW	0	– 24.5	0.8	27.5	2.46E+07	0.0427	0.2
CWa	0	– 16.1	0.8	13.7	1.74E+07	0.0427	0.2
CWb	– 16.1	– 24.5	0.8	27.5	2.46E+07	0.0427	0.2

Table 9 Excavation sequence of the 3D simulation

Phase	Activity	Remarks
1	Excavation to GL.–2.1 m	First exc. stage
2	Strut installed at GL.–1.2 m	H400 × 400 × 13 × 21 Preload: 750 kN/ea
3	Excavation to GL.–5.6 m	Second exc. stage
4	Strut installed at GL.–4.7 m	H400 × 400 × 13 × 21 Preload: 2 × 800 kN/ea
5	Excavation to GL.–9.1 m	Third exc. stage
6	Strut installed at GL.–8.2 m	H400 × 400 × 13 × 21 Preload: 2 × 800 kN/ea
7	Excavation to GL.–13.2 m	Fourth exc. stage
8	Strut installed at GL.–12.3 m	H428 × 407 × 20 × 35 Preload: 2 × 1250 kN/ea
9	Excavation to GL.–16.1 m	Final exc. stage

Note: "ea" denotes "each strut"

5.2 Numerical Results

The wall displacements at the end of excavation by numerical analysis were presented in Fig. 15 together with the field measurements. It is found that the calculated and measured wall displacements were both small, but there was little resemblance on the shape of displacement curves. Since there are so many undocumented construction details that may affect the behavior of diaphragm wall during excavation, no attempt was made to better fit the field curves. Of course one can always fit the field measurements to certain extent by back-analysis technique, but it is suspected that the back-analyzed parameters would be too far away from realistic for this case history. As the input parameters had not been massaged to mimic the field curves, the numerical analysis can be classified as a Type I blind prediction.

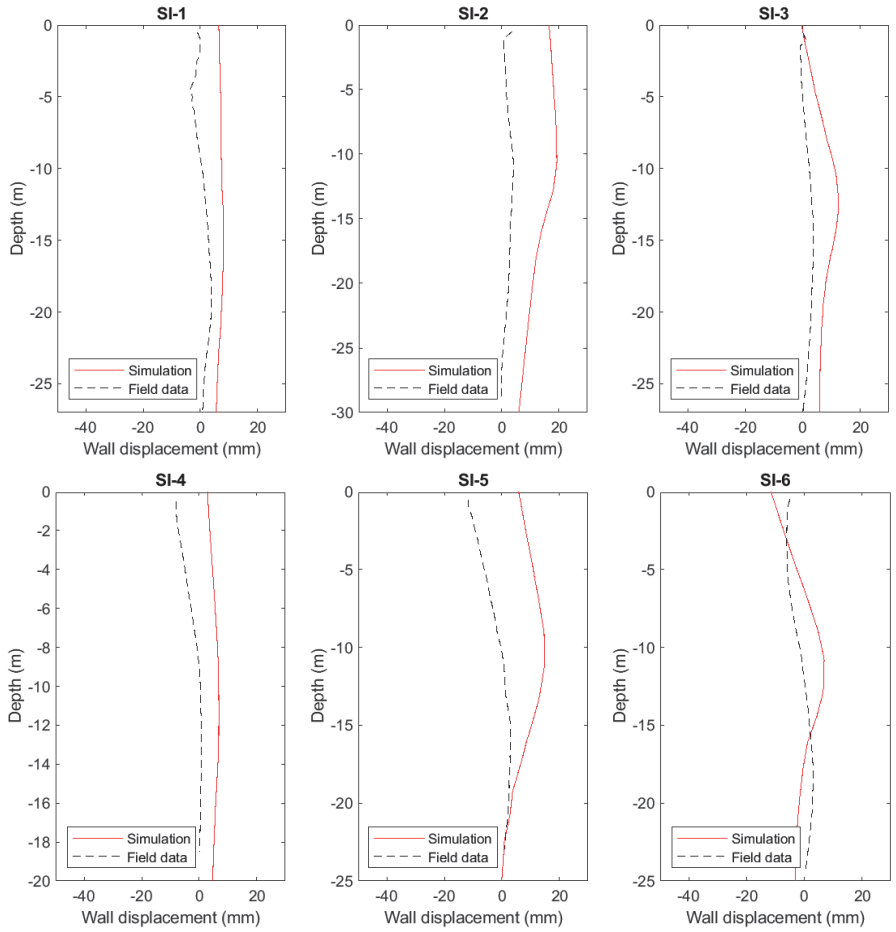

Fig. 15 The comparison of measured and computed wall displacements

The numerical results, field measurements, predictions by Clough's original scheme and predictions by the revised scheme are summarized in Table 10 for comparison. When compared with the results from Clough's original scheme, it was found that the numerical results are much more comparable to the numbers obtained by the revised scheme. This is an indication that the revised scheme is capable of better predicting the wall displacement for excavations in soft clay strengthened with cross walls.

It is evident in Tables 6 and 10 that δ_{Clough}, δ_{rev}, and δ_{3D} all exceed δ_{field} by a large magin. In average, δ_{Clough}, δ_{rev}, and δ_{3D} are about 84, 14, and 4 times the magnitude of δ_{field}, respectively. Since Clough's original scheme ignores the cross walls and corner effects, the over estimation of δ_{Clough} on δ_{field} is reasonably understood. With a little surprise, δ_{rev} still over predicts the wall displacement by an order of 10, perhaps the effects of cross walls and corners are only partially incorporated by the current approaches.

Table 10 Comparison of predicted wall displacements and 3D results with field measurements

SI	δ_{field} mm	δ_{clough} (mm)	δ_{rev} (mm)	δ_{3D} (mm)	δ_{clough} / δ_{field} (–)	δ_{rev}/ δ_{field} (–)	δ_{3D} / δ_{field} (–)
1	3.90	209.30	27.25	8.15	53.67	6.99	2.09
2	4.11	177.10	34.60	19.28	43.09	8.42	4.69
3	3.78	206.08	28.04	12.45	54.52	7.42	3.29
4	0.83	177.10	31.01	6.85	213.37	37.36	8.25
5	3.01	209.30	30.93	14.87	69.53	10.28	4.94
6	3.04	209.30	40.80	6.91	68.85	13.42	2.27

To the biggest surprise of all, δ_{3D} still falls in the range of about 4 times the field magnitude, though 3D analysis is believed to best model the real situation. As stated in Section 4.5, there may be field activities that cannot be fully simulated in the 3D analysis, but those simplifications should not have accumulated to a discrepancy of 4 times. A close observation of the 3D results reveals that the predictions of wall displacement on all 6 inclinometer casings exceed a factor of at least 2, which is a systematical overprediction that is perhaps the nature of this particular project. The authors also suspect that field engineers might have done a superb job in limiting the average wall displacements to a level near 0.02% of the excavation depth (0.03 m/16 m), which outperformed all predictions by a wide margin. In fear of further damaging the fragile adjacent buildings, the mentality of field engineers is very conservative, that is probably why the measured wall displacements are controlled at such a low level, and this extremely low displacement level should not be considered as a norm for similar projects. In summary, the revised scheme provides much improved results over the original scheme; however, the revised predictions still deviate from the 3D and field results by a significant margin.

5.3 Sensitivity Study on Clay Strength

A parametric study was carried out to investigate the sensitivity of wall displacement on clay strength. Varying the undrained shear strength of clay from $s_u = 0.18\sigma_v'$ to $s_u = 0.32\sigma_v'$, the wall displacements were calculated by PLAXIS 3D and presented in Fig. 16. The difference of maximum wall displacements for s_u =

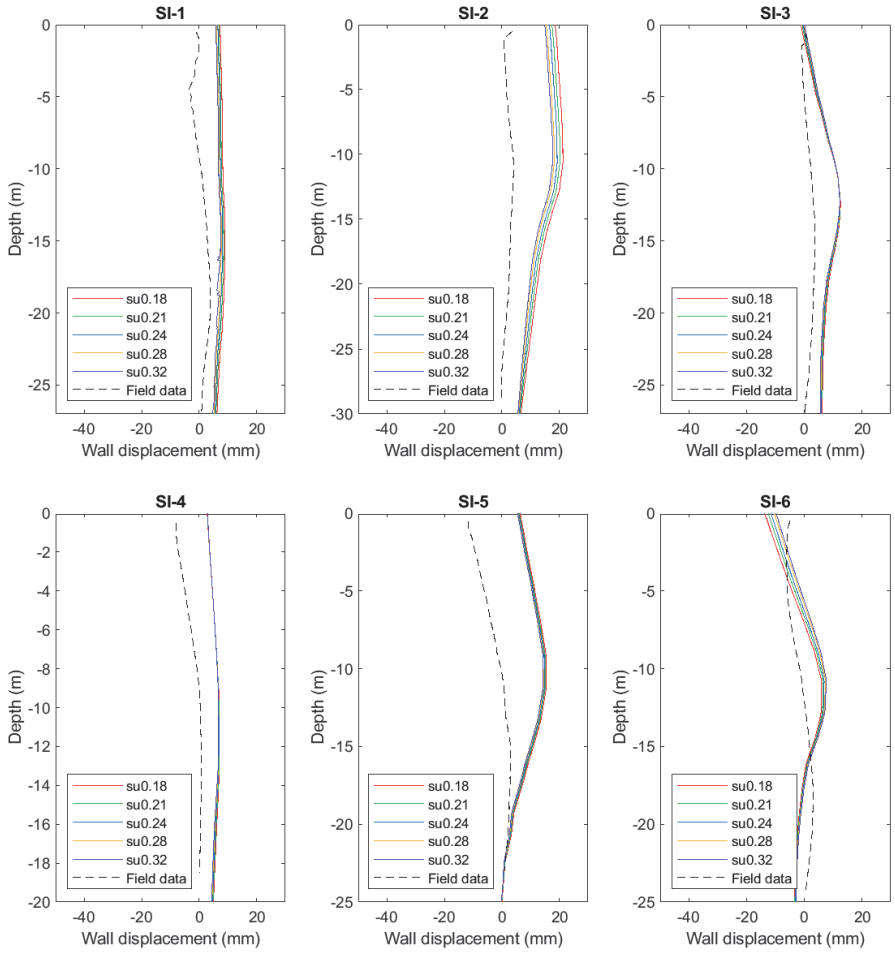

Fig. 16 Variation of the computed wall displacements with varying undrained shear strength of clay

$0.18\sigma_v'$ and $s_u = 0.32\sigma_v'$ are not discernible as all these numerical results seem to merge into one single curve as shown in Fig. 16. This finding is against design experience for excavations in soft clay, as the calculated wall displacement is very sensitive to the variation of s_u, a small variation of s_u may lead to a tenfold increase of the calculated displacement. In summary, these results imply that the cross walls in this particular case may have a dominant effect on wall behavior, reducing the clay strength by more than half only leads to an insignificant increase in wall displacement.

5.4 Sensitivity Study on Strut Stiffness

Another numerical test using 50% of the strut stiffness and 50% of the preload together with the original clay strength was also carried out, and the results are presented in Fig. 17. As indicated in Fig. 17, the difference in wall displacement for each inclinometer casing is also insignificant. A plausible explanation for this finding is that the strengthening effects of cross walls overshadowed the effect of strut rigidity. In other words, the excavation behavior of this particular project is controlled by the effects of cross walls.

6. DISCUSSIONS

The presence of cross walls would increase the overall stiffness of the retaining system without a doubt; the question is how this strengthening effect can be quantified. The concept of combined system stiffness and adjusted factor of safety against basal heave more or less captures the contribution of cross walls in limiting the diaphragm wall displacement. Though the preliminary study showed comparable results between the predicted displacements, numerical results and field measurements of this case history, the concept of combined system stiffness and adjusted factor of safety against basal heave is still far from perfect. At this stage, the combined system stiffness and adjusted factor of safety against basal heave can at best be regarded as indices to characterize the overall stiffness of the retaining system strengthened by cross walls; much more researches are obviously required to further revise the proposed schemes. The effects of other auxiliary measures to strengthen the retaining system, such as buttress walls and soil improvement, also deserve attention and may have to be quantified in a later stage.

For this particular case history, it appears that the cross walls have a dominant effect on the behavior of diaphragm wall as the numerical results showed little variation of the wall displacements even if the shear strength of clay and stiffness of bracing system are dramatically reduced. One implication is that the cross walls were over designed and the number of cross walls could have been reduced. However, the cross walls in this case history mainly served as load bearing elements to support the structural weight, therefore the layout of cross walls was determined by structural requirement rather than excavation concerns. As this is the norm, the cross walls for most projects serve a dual purpose to minimize wall displacement as well as to control foundation settlement.

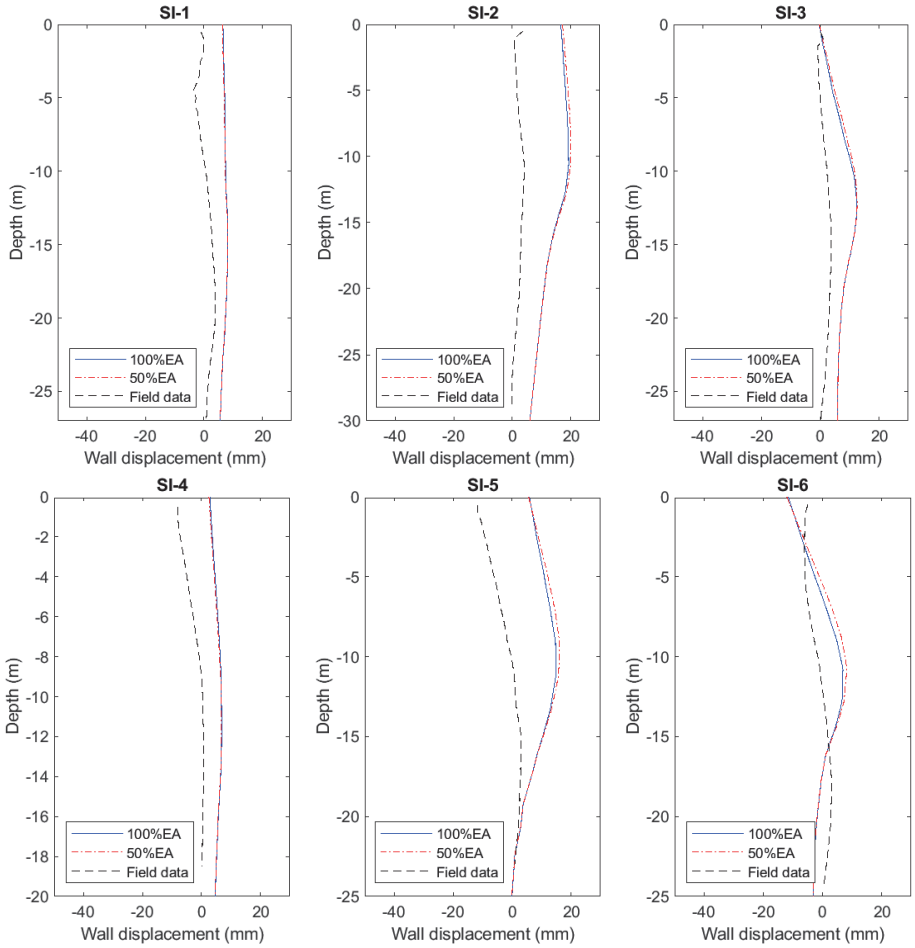

Fig. 17 Profiles of wall displacement at 50% bracing stiffness

Another interesting feature to note is the extended design curves are almost flat straight lines in areas with high system stiffness and high factor of safety against basal heave. This implies that if wall displacement is of concern, there is no need to further increase the system stiffness and factor of safety against basal heave once these two parameters reach threshold values. It is also observed in these areas the wall displacement can reach as low as 0.02% to 0.12% of the excavation depth. For practical design purpose, 0.12% of the excavation depth can be regarded as the lower limit of the designed wall displacement. Noting that the two parameters $F_b \geqq 3$ and $S \geqq 3000$ are rarely obtainable for most excavations in soft clay with less amount of cross walls such as the one adopted in this case history, it can perhaps be concluded that the theoretically achievable minimum wall displacement is about 0.12% of the excavation depth. Though field measured wall displacement can reach as low as 0.02% of the excavation depth, it is probably not a good practice to design the retaining system at such a low displacement level, a certain level of conservativeness should always be observed for deep excavation in soft clay.

A simple equation that relates the maximum wall displacement to system stiffness and factor of safety against basal heave is derived and presented in this paper. This equation is the best-fit and extrapolation of the original design curves which enables the engineers to estimate the wall displacement further into the area of high system stiffness and high factor of safety against basal heave. That is to say, the blur lower right corner of Clough's original graph where the wall displacement level is extremely low is now better focused. Together with the schemes to quantify the effects of cross walls, this equation allows engineers to easily tinker with the design of cross walls instead of resorting to a complicated numerical analysis.

7. CONCLUSIONS

This paper presents a deep excavation case history in soft clay with its retaining system strengthened by cross walls. The observed wall displacements are at an extremely low level that they obviously exceed the applicable range of Clough's original graph. In an effort to remedy this shortcoming, Clough's original design curves are extended by extrapolation technique to cover excavations with high system stiffness and high factor of safety against basal heave. The effects of cross walls on system stiffness and factor of safety against basal heave are quantified by invoking the concepts of plane strain ratio and equivalent soil strength, respectively. As a result, the combined system stiffness and adjusted factor of safety against basal heave are adopted as the new parameters to represent the characteristics of a deep excavation in soft clay with cross walls. Using the extended design curves together with these two revised parameters, the predicted wall displacements are in much better agreement with the field observation and numerical results than the original prediction by Clough's scheme. It is therefore concluded that the revised schemes and the extended design curves have the potential to serve as a reliable tool in estimating the wall displacements for excavations with cross walls in soft clay.

NOTATIONS

A	Cross sectional area (m^2)
B	Width of excavation (m)
c	Cohesion of soil (kN/m^2)
c'	Effective cohesion (kN/m^2)
E	Young's modulus (kN/m^2)
EA	Axial stiffness of strut (kN)
EI	Flexural rigidity of retaining wall ($kN\text{-}m^2$)
F_b	Factor of safety against basal heave
F_{b_adj}	Adjusted factor of safety against basal heave (effect of cross walls included)
f_c'	Strength of concrete (kN/m^2)
H_e	Excavation depth (m)
h_{avg}	Average vertical spacing between supports (m)
I	Moment of inertia (m^4)
L	Length of excavation, or length of perimeter diaphragm wall reinforced by the cross walls (m)
L_{cw}	Length of cross wall (m)
N	Blow count of standard penetration test
N_{cw}	Number of cross walls
PSR	Plane strain ratio
R_{int}	Interface reduction factor
S	System stiffness
S_c	Combined system stiffness
SI	Notation for inclinometer casing
s_u	Undrained shear strength of soft clay (kN/m^2)
s_{ub}	Average undrained shear strength below dredge line (kN/m^2)
s_{uu}	Average undrained shear strength above dredge line (kN/m^2)
s_{ub}^*	Equivalent undrained shear strength below dredge line (effect of cross walls included) (kN/m^2)
s_{ub_adj}	Average value of s_{ub}^* and s_{ub} (kN/m^2)
α	Factor of regression equation for S and F_b
β	Adhesion factor for cross wall
ϕ'	Effective friction angle (°)
γ_t	Total unit weight of soil (kN/m^3)
γ_w	Unit weight of water (kN/m^3)
ν	Poisson's ratio
ν_u	Poisson's ratio for undrained analysis
σ_v'	Effective overburden pressure (kN/m^2)
δ_{field}	Measured maximum wall displacements (mm)
δ_{Clough}	Maximum wall displacements predicted by Clough's original scheme (mm)
δ_{hm}	Maximum wall displacement (mm)
δ_{rev}	Maximum wall displacements predicted by revised scheme (mm)
δ_{3D}	Maximum wall displacements predicted by 3-dimensional numerical analysis (mm)

REFERENCES

Bryson, L.S. and Zapata-Medina, D.G. (2012). "Method for estimating system stiffness for excavation support walls." *Journal of Geotechnical and Geoenvironmental Engineering,* ASCE, **138**(9), 1104-1115. https://doi.org/10.1061/(ASCE)GT.1943-5606.0000683

Clough, G.W., Smith, E.M., and Sweeney, B.P. (1989). "Movement control of excavation support systems by iterative design." *Proceedings of ASCE Foundation Engineering: Current Principles and Practices*, **2**, 869-884.

Finno, R.J., Blackburn, J.T., and Roboski, J.F. (2007). "Three-dimensional effects for supported excavations in clay."

Journal of Geotechnical and Geoenvironmental Engineering, ASCE, **133**(1), 30-36. https://doi.org/10.1061/(ASCE)1090-0241(2007)133:1(30)

Hsieh. P.G. and Ou, C.Y. (1998). "Shape of ground surface settlement profiles caused by excavation." *Canadian Geotechnical Journal*, **35**(6), 1004-1017. https://doi.org/10.1139/cgj-35-6-1004

Hsieh, H.S. and Lu, F.C. (1999). "A note on the analysis and design of diaphragm wall with buttresses." *Sino-Geotechnics*, **76**, 39-50 (in Chinese). https://doi.org/10.30140/SG.199912.0002

Hsieh, H.S., Lu, Y.C., and Lin, T.M. (2008). "Effects of joint details on the behavior of cross walls." *Journal of GeoEngineering*, **3**(2), 55-60. https://doi.org/10.6310/jog.2008.3(2).2

Hsieh, H.S., Hsu, W.T., and Chou, C.J. (2015), "Incorporating 3-dimensional effect in the design of a small excavation in soft clay." *Proceedings* of *International Conference on Soft Ground Engineering*, Singapore, 669-677.

Ou, C.D, Shih, C., and Hsieh, H.S. (1988). "Design of diaphragm wall as retaining structure for deep excavation: models and guidelines." *Sino-Geotechnics*, **21**, 10-17 (in Chinese).

Ou, C.Y., Chiou, D.C., and Wu, T.S. (1996). "Three-dimensional finite element analysis of deep excavations." *Journal of Geotechnical Engineering,* ASCE, **122**(5), 337-345. https://doi.org/10.1061/(ASCE)0733-9410(1996)122:5(337)

Ou, C.Y., Lin, Y.L., and Hsieh, P.G. (2006). "Case record of an excavation with buttress walls and cross walls." *Journal of GeoEngineering,* **1**(2), 79-86. https://doi.org/10.6310/jog.2006.1(2).4

PLAXIS (2013). *PLAXIS 3D Computer Software*. Delft, Netherlands, PLAXIS.

Terzaghi, K. (1967). *Theoretical Soil Mechanics*, John Wiley & Sons, New York. http://dx.doi.org/10.1002/9780470172766

TORSA (2016). *Taiwan Originated Retaining Structure Analysis,* Sino-Geotechnics Research and Development Foundation (computer code).

TORSA3 (2019). *Taiwan Originated Retaining Structure Analysis, Version 3,* Sino-Geotechnics Research and Development Foundation (computer code, English version), to be released.

Woo, S.M. and Moh, Z.C. (1990). "Geotechnical characteristics of soils in the Taipei basin." *Proceedings of the 10th Southeast Asian Geotechnical Conference*, **2**, Special Taiwan Session, 51-65.